Coherent surface phonon at a GaAs(100)-$c(8\times2)$ surface

Kazuya Watanabe, Dimitre T. Dimitrov, Noriaki Takagi, and Yoshiyasu Matsumoto*
Department of Photoscience, School of Advanced Sciences, The Graduate University for Advanced Studies (Sokendai), Hayama, Kanagawa, 240-0193, Japan

(Received 24 January 2002; published 20 June 2002)

Coherent surface phonon at a GaAs(100)-$c(8\times2)$-Ga reconstructed surface has been investigated by time-resolved second-harmonic generation (TRSHG). The phonon mode is impulsively excited by an ultrashort laser pulse and subsequent coherent nuclear motion is monitored through the intensity modulation of the second harmonics of a probe pulse. Oscillatory traces are clearly observed in TRSHG signals and their Fourier transformation show two peaks at 8.2–8.6 and 8.9 THz. Fitting these traces with two oscillatory components shows that the oscillatory signals are contributed by the bulk LO phonon at 8.8 THz and the surface phonon at 6.0–8.6 THz. The relative amplitude of the surface phonon modes is sensitive to sputtering and annealing of the surface. Clear dips appear at 8.7 THz in the Fourier spectra, which is caused by the initial phase difference between the surface phonon and the bulk phonon modes. The frequency of the surface component shows red shifts as the pumping power increases. The shifts are indicative of a marked electron phonon interaction or anharmonicity of the surface phonon modes.

DOI: 10.1103/PhysRevB.65.235328 PACS number(s): 68.35.Ja, 78.47.+p, 78.68.+m

I. INTRODUCTION

There has been an accumulating body of literature dealing with generation of coherent nuclear motion by ultrashort optical pulses not only in the gas phase[1] but also in various kinds of condensed phases.[2–4] Laser pulses with the duration sufficiently shorter than the period of a vibrational mode allow us to excite the mode with a high degree of spatial and temporal coherence and to follow the nuclear motion directly in the time domain. Moreover, it has been demonstrated that successive multiple pulse trains enhance selectively the coherent amplitude of a specific mode.[5–7]

These unique features of the coherent excitation provide an attractive opportunity for the study of surface reaction dynamics. Surface reactions are generally initiated by the excitation of surface phonons and adsorbate vibrations. If we obtain detailed information on the dynamics of nuclear motions of surface atoms, we can gain a deeper insight into what vibrational motions are relevant to a reaction. Furthermore, the selective enhancement of a surface phonon mode relevant to the reaction may lead us to control the surface reaction dynamics. For this purpose, it is necessary to establish the method to excite and probe the coherent nuclear motion at a surface.

In contrast to a number of works on coherent bulk phonon excitation reported,[3] studies on the excitation of coherent phonons or vibrations at surfaces are scarce. Recently, Chang *et al*. have pioneered the probe of the coherent surface phonon modes at a GaAs surface and a buried interface by use of time-resolved second-harmonic generation (TRSHG).[8–10] They have succeeded in observing coherent surface phonons at the surfaces of GaAs(110), GaAs(100)-(4×1)-Ga, and GaAs(100)-(6×1)-As in the time domain. Several surface phonon modes were identified on each surface. In addition, an interface phonon mode between GaAs(100) and native oxide layers was observed.[9]

To extend this technique further for the study on surface chemical reaction dynamics, one has to examine carefully the nature of the coherent surface phonon excited by this method in detail. For example, it is important to know how the coherent amplitude depends on the excitation laser intensity. Information on the initial phase of the coherent oscillation is valuable for the excitation mechanism. However, these issues have not been discussed extensively in the previous works.

In this work, we focus on TRSHG on a GaAs(100)-$c(8\times2)$-Ga surface. Although some results have been reported by Chang *et al.* on the clean GaAs(100) surfaces,[10] no study on the $c(8\times2)$-Ga reconstructed surface has been done. This paper describes new features in TRSHG traces of this surface that has not been reported in the pervious works. We show a clear interference dip in the Fourier power spectra of the TRSHG traces, which is indicative of the initial phase difference between the bulk and the surface coherent phonon modes. In addition, the contribution of the surface phonon modes depend significantly on the annealing time of the sample, indicating that the observed modes are laterally well delocalized at the surface. Furthermore, we show the red shift of the surface phonon frequency with increasing the excitation laser power and discuss its possible origins.

II. EXPERIMENT

Figure 1 shows a schematic diagram of the experimental setup used in this study. The experiment was performed with a UHV chamber evacuated to a base pressure better than 3.0×10^{-10} Torr by cascaded turbo-molecular pumps. It is equipped with a retractable LEED and a retractable cylindrical mirror analyzer for Auger electron spectroscopy (AES). A GaAs(100) sample (*n*-type, Si-doped, $1-5\times10^{18}$ cm^{-3}) was held by a Ta foil welded to Ta wires. It could be heated up to 1000 K by resistive heating of the Ta wires, and could be cooled down to 110 K by liquid nitrogen. Sample was cleaned by cycles of Ar^+ sputtering (1 μA, 500 V) and annealing. The surface condition was checked by LEED and AES. After the cleaning procedure the surface contamination

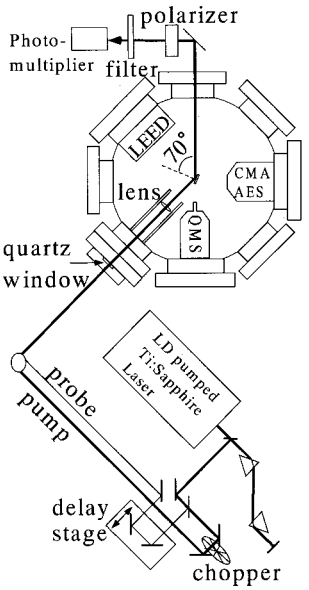

FIG. 1. Schematic diagram of a TRSHG experimental setup.

of carbon and oxygen was under the detection limit of AES (less than a few % of surface atoms). A GaAs(100)-$c(8\times2)$-Ga reconstructed surface was obtained by annealing the sputtered surface to higher than 900 K.

TRSHG signals were measured by basically the same method reported by Chang *et al.*[8–10] We used a chirped-mirror-compensated femtosecond Ti:sapphire laser (Femtosource, Femto-pro, 800 nm, 12 fs; 75 MHz, 800 mW) as a light source. The output laser beam was passed through a prism pair for compensating further chirping by optical components mounted between the laser and the sample. A part (30%) of the output beam was used as a probe beam, and the rest was passed through a variable neutral density filter and used as a pump beam. The time delay t between the pump and the probe pulses was controlled by a computer-controlled mechanical mirror stage with the accuracy of better than 10 fs. The pump and the probe beams were introduced in the chamber in parallel to each other with a spacing of 7 mm through a window of a 1-mm-thick quartz plane plate (the aperture diameter of 20 mm). Then both of the beams were focused onto the sample surface by a quartz lens of the 100-mm focal length held in the chamber. The incidence angles of the two beams onto the sample surface were ~70°. The electric vectors of the beams were in the incidence plane (p polarization) parallel with the [0–11] direction. The p-polarized component of the second harmonics (SH) of the probe beam generated on the sample surface was passed through a band pass filter to reject the fundamental light and detected by a photomultiplier thermoelectric-cooled down to −30 °C. The output signal of the photomultiplier was amplified by a current preamplifier and fed into a lock-in amplifier synchronized with an optical chopper that was inserted in the optical path of the pump beam. Pump-pulse induced changes of the SH intensity were recorded as a function of the pump-probe delay from −0.2 to 6 ps with a step of 26 fs. The time zero was determined by monitoring SH light produced by sum frequency generation of the pump and the probe pulses. The sample temperature was kept at 180 K during the measurements.

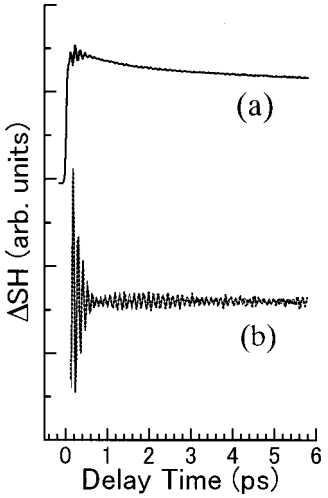

FIG. 2. (a) A typical TRSHG trace taken from a GaAs (100)-$c(8\times2)$ surface. The pump power was 140 mW, and the SH signal with p polarization was detected. The incidence plane was parallel to [0-11] direction. (b) Dotted curve: A derivative curve of the trace (a). Solid curve: a simulation curve with two components α and β in Eq. (2). See text for the parameters employed in the simulation.

III. RESULTS

Figure 2(a) shows a typical TRSHG trace obtained on the GaAs(100)-$c(8\times2)$-Ga surface. A clear oscillatory component is superimposed on the background component with a rapid rise and a slow decay. The derivative of the curve in Fig. 2(a) is plotted in Fig. 2(b) after subtracting low frequency (<3 THz) components. While a large amplitude oscillation component appears immediately after the excitation pulse almost decays within $t<1$ ps, a small oscillation component is persistent in $t>1$ ps.

The transient changes are due to the modulation of the effective second-order nonlinear susceptibility $\chi^{(2)}$ by the pump pulses. The origin of the $\chi^{(2)}$ photomodulation has been discussed by Chang *et al.*[10] Since a bulk GaAs crystal lacks an inversion symmetry, SHG signals are contributed both from the bulk and the surface. The pump pulse excitation induces the changes in the population distributions of electron and hole in surface electronic bands as well as in bulk bands, resulting in the modulation of $\chi^{(2)}$. In addition, the electric field in a depletion layer near the surface of a semiconductor also contributes SHG signals.[11] In this case, the responsible nonlinear dipole is proportional to $E_{\mathrm{dep}}\chi^{(3)}$, where E_{dep} is the strength of the depletion field and $\chi^{(3)}$ is the third-order nonlinear susceptibility. Photocarriers generated by the pump pulse modify E_{dep} by screening, and thereby cause the modulation of the SH intensity. Therefore, the background component with the rise and the decay apart from the oscillatory one in Fig. 2(a) reflects the photocarrier dynamics near the surface region including electron-hole generation, screening, diffusion, trapping at surface states, and recombination.

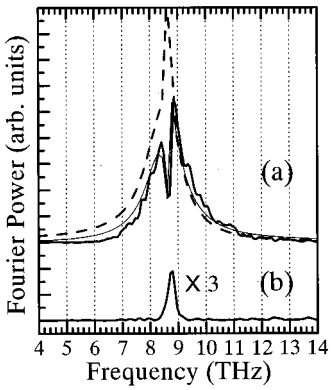

FIG. 3. The power spectra obtained from the Fourier transformations of the TRSHG traces in Fig. 2(b). (a) The transformation is performed for the data in the range from 70 fs to 5.8 ps of the measured (thick curve) and the simulated (thin curve) traces. The dashed curve represents also the simulated results with the same parameter set for the thin curve except that the initial phases of the components α and β are set to be equal ($\phi_1=\phi_2=-12°$). (b) The power spectrum obtained from the experimental data in Fig. 2(b) in the range from 1.0 to 5.8 ps.

Coherent nuclear motion induced by the ultrashort pulse excitation also modulates the SH intensity via hyper Raman tensors $\delta\chi^{(2)}/\delta q_l$, where q_l stands for the normal coordinate of the lth bulk or surface phonon mode. Since the modulation of the SH intensity by the coherent nuclear motion under the present excitation condition is considered to be small (a few percent of the total SH intensity) on GaAs surfaces, the signal quadratic to the nuclear displacement would be hardly detected. Thus, the observed oscillatory contribution in Fig. 2(a) would be linear to the nuclear displacement.

The coherent phonon oscillation can be described phenomenologically by the equation of motion of the displacement amplitude Q expressed as[12]

$$\mu^*\left[\frac{\partial^2 Q(t)}{\partial t^2}+2\gamma_d\frac{\partial Q(t)}{\partial t}+\omega^2 Q(t)\right]=F(t), \qquad (1)$$

where ω is the phonon frequency, μ^* is the lattice reduced mass, γ_d is a phenomenological damping constant, and $F(t)$ is the appropriate driving force. When $F(t)$ is assumed as a delta function and $\gamma_d \ll \omega$ is satisfied, one obtains a solution for an underdamped mode with the frequency of ω and the decay time of $1/\gamma_d$. The decay time is contributed by a pure dephasing (transverse relaxation) rate and a population decay (longitudinal relaxation) rate. In addition, when more than two distinct modes overlap each other in the frequency domain, this imhomogeneous broadening increases the decay rate of the coherent amplitude.

Power spectra are obtained by Fourier transformation of the derivative curve in Fig. 2(b). Here we plot the power in two different time domains: one in the range from 70 fs to 5.8 ps in Fig. 3(a) and the other from 1.0 to 5.8 ps in Fig. 3(b). Two peaks at 8.9 and 8.4 THz are prominent and a sharp dip at 8.7 THz appears in Fig. 3(a). On the other hand, the power spectrum of a longer delay times after the rapid

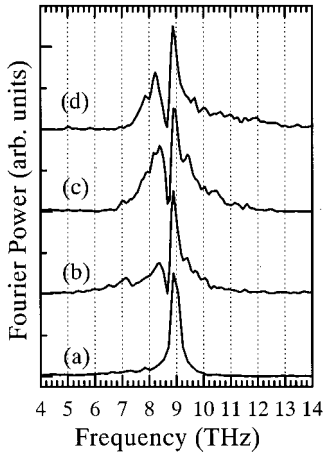

FIG. 4. The Fourier power spectra of TRSHG curves under various surface conditions: the TRSHG curves were observed after the Ar^+ sputtering (a) without annealing the surface, (b) 1 h annealing at 950 K after the sputtering, (c) 2 h annealing, and (d) 3 h annealing.

damping of the initial large oscillation [Fig. 3(b)] shows only one peak at 8.8 THz. The frequency of a bulk LO phonon was reported to be 8.8 THz by time-resolved linear reflectivity measurements of GaAs.[13] Chang *et al.* have also observed the bulk LO-phonon peak at 8.8 THz in the TRSHG measurements,[10] in addition to the four surface phonon modes in the region of 6.2–8.2 THz. Thus the peaks at 8.9 and 8.4 THz could be assigned to the bulk LO phonon and a surface phonon, respectively. However, some obscure points remain. The peak at 8.9 THz is quite asymmetric as in Fig. 3(a), but becomes symmetric and its peak position is slightly shifted as in Fig. 3(b). In addition, no surface phonon component peaked at 8.4 THz was observed by Chang *et al.* at GaAs(100)-(4×1)-Ga nor-(1×6)-As surfaces.[10]

In order to clarify these points, we simulated the observed oscillatory traces $D(t)$, with a linear combination of two underdamped modes, as in Eq. (2):

$$D(t)=A_1\sin(\omega_1 t+\phi_1)\exp(-t/\tau_1)+A_2\sin(\omega_2 t+\phi_2)\times\exp(-t/\tau_2). \qquad (2)$$

A simulated curve (solid curve) is superimposed on the measured data in Fig. 2(b). The employed parameters are as follows: $\omega_1=8.67$ THz, $\tau_1=3$ ps, $\phi_1=-12°$, $\omega_2=8.52$ THz, $\tau_2=0.22$ ps, $\phi_2=-128°$, and $A_1:A_2=1:23$. The power spectrum of the simulated curve is also plotted in Fig. 3(a). It is obvious that the essential features of the oscillatory curve measured by TRSHG are well represented by a linear combination of the two underdamped oscillators. Hereafter we denote the first one as the α component that has a decay time of about 3 ps and a center frequency at 8.7 THz, and the second one as the β component that has a decay time of 220 fs and a center frequency at about 8.5 THz.

Note that the initial phase of the α components (ϕ_1) is shifted relatively from that of the β component (ϕ_2) by about 120°. The relative phase shift is crucial to obtain the satisfactory simulation of the waveform. The dashed curve in

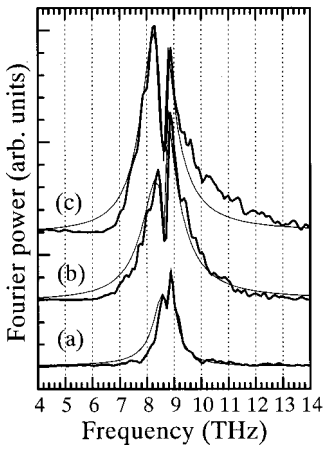

FIG. 5. The pump power dependence of the Fourier power spectra of TRSHG traces. Thick curves represent the results taken from the surface with 3 h annealing after the Ar^+ sputtering. The pump power for each curve is (a) 70 mW, (b) 140 mW, and (c) 210 mW, respectively. Thin curves represent the results simulated by the two components analysis with Eq. (2). The used parameters for the components α and β are tabulated in Table I.

Fig. 3(a) shows a spectrum of a simulated oscillatory trace with the same parameters as those for Fig. 2(b) except that the initial phases of the two components are set to be equal ($\phi_1=\phi_2=-12°$). In this case, the characteristic dip at 8.7 THz in the power spectrum disappeared and the two peaks are collapsed into one broad peak. Therefore, it is clear that the asymmetric spectral shape and the slight frequency shift of the peak at 8.9 THz and a dip at 8.7 THz in Fig. 3(a) are due to the interference between the α and the β components. We will discuss the physical origins of the initial phase difference of the two components in detail later.

TRSHG waveforms significantly depend on how the surface is prepared. Figure 4 shows a series of power spectra obtained with various annealing times after Ar^+ sputtering (500 eV, 1 μA, for 5 min, at 270 K). Right after the sputtering the surface showing a diffuse (1×1) LEED pattern we observed only the peak at 8.9 THz; the peak at 8.4 THz is strongly reduced. As the total annealing time after the sputtering increases, the spectral feature at 7–8.6 THz grows, and finally results in a peak at 8.4 THz. The surfaces giving the traces in Figs. 4(b)–4(d) all show almost the identical $c(8\times2)$ pattern. From the two-component quantitative analysis, we can understand the surface condition dependence of the spectra as follows; the amplitude of the β component decreases by the surface sputtering and recovers by the annealing. Thus, it is likely that the β component is originated in excitation localized in a few layers near the surface.

Figure 5 shows the excitation power dependence of the power spectra. The sample was annealed at ~950 K for 3 h after sputtering [the condition identical with that of Fig. 4(d)]. At the lowest pump power of 70 mW, two peaks appear at 8.6 and 8.9 THz, and as the pump power is increased, the lower frequency peak increases in its relative intensity and are shifted to red. All the waveforms under the three different pump power conditions could be reproduced qualitatively by a linear combination of two underdamped oscillators, Eq. (2). The power spectra of these simulated curves are also shown in Fig. 5. The parameters used for the simulations are tabulated in Table I. In the simulated curves, the α component is always with a decay time of 2–3 ps and with a center frequency of 8.7–8.8 THz. Differences of the initial phases of the α and β components are 69°, 116°, and 103° for pump power of 70, 140, and 210 mW, respectively, and these phase differences give a dip at 8.7 THz in each spectrum.

IV. DISCUSSION

A. Origins of the oscillatory components

The observed features of the oscillatory signals apparent in the TRSHG traces are summarized as follows. The oscillatory parts are decomposed into two underdamped modes: the components α and β. The α component has a frequency of 8.7–8.8 THz and a decay time of 2–3 ps, and appears irrespective of the surface sputtering and annealing, and the pump power. Thus, this component is assigned to the bulk LO-phonon mode. On the other hand, the β component has a center frequency lower than that of the α component, and possesses much shorter decay times (200–400 fs). The β component is reduced by surface sputtering and recovers its intensity by annealing. Thus, the β component is very sensitive to long-range regularity of the surface. In addition, the β component changes its frequency and the width (decay time) as a function of the pump power.

There are some candidates for the origin of the β component: surface phonon, and the bulk plasmon-bulk phonon coupled mode. Here we first discuss the possibility of the bulk plasmon-bulk phonon coupled modes. The coherent oscillation of the electron plasmon-bulk LO-phonon coupled

TABLE I. Parameters used for the simulations in Fig. 5.

	α component		β component		
Pump power (mW)	Center frequency (THz)	Decay time (ps)	Center frequency (THz)	Decay time (ps)	Initial phase difference between α and β (deg.)
70	8.80	2.8	8.65	0.40	69
140	8.67	3.0	8.52	0.22	116
210	8.66	2.3	8.34	0.24	103

mode has been observed by transient linear reflection measurements on GaAs.[14,15] Its lower (L_- mode) and the higher branch (L_+ mode) change their frequencies from 7 to 8 THz (L_-) and from 10 to 15 THz (L_+) as the carrier concentration increases from 1×10^{17} cm^{-3} to 1×10^{18} cm^{-3}. In the current study, the penetration depth of the pump light is estimated to be about 1.5 μm. The injected carrier densities averaged in the penetration depth are 4.3, 8.6, and 13 $\times10^{17}$ cm^{-3}, at the pump power of 70, 140, and 210 mW, respectively. On the other hand, the depth of the surface region contributing to the SH signal is estimated to be ~130 Å from the phase matching condition. The injected carrier densities averaged in the narrow region are in the range from 6.6 to 20×10^{17} cm^{-3}. The frequency of the β component does not mach to those of the electron plasmon-phonon coupled modes expected for those carrier densities. Furthermore, the reduction of the β component by sputtering indicates that this component is sensitive to the topmost 10–20 Å layer of the surface, where the contribution from the bulk mode would be small. Therefore, the β component is not likely due to the electron plasmon-bulk LO-phonon coupled modes.

Wan *et al.* have observed a bulk LO-phonon–hole plasmon coupled mode of *p*-type GaAs by Raman spectroscopy in the range from 8.0 to 8.8 THz depending on the hole density.[16] The peak frequency of the coupled mode shifts from 8.8 to 8.0 THz as the hole density changes from 1 $\times10^{18}$ to 1×10^{19} cm^{-3}. Although the β component shows the similar frequency shift as a function of the pump power, the employed carrier densities in the current study are almost one order of magnitude smaller than those reported in Ref. 16. Furthermore, the reduction of the mode by surface sputtering cannot be explained by the bulk-phonon–hole-plasmon coupled mode.

Next, we examine if the surface phonon modes are responsible for the β component. In a HREELS study on a GaAs(100)-$c(8\times2)$ surface, the peaks at 7.9, 11.5, and 35.8 meV (1.91, 2.78, and 8.66 THz, respectively) have been observed.[17] The frequency of the highest mode ascribed to the Fucks-Kliewer (FK) mode is close to that of the β component. However, since the lateral wave vector of the FK mode to be excited in the present study should be smaller than 1 μm^{-1}, the FK mode extends more than 1 μm into the bulk.[18] Such a bulklike mode should be insensitive to the modification of the surface. Thus, if this bulk like mode were responsible for the β component, it would be difficult to understand why the β component is so sensitive to surface sputtering and annealing. The absence of the contribution of the FK mode in TRSHG measurements has been also claimed by Chang *et al.*[8–10] Consequently, we conclude that the β component is due to surface phonon modes localized in a few atomic layers near the surface.

We have tentatively assumed so far that the β component is composed of one damped oscillator. However, the spectral width of the β component is rather broad and its decay time is much shorter than that of the bulk LO phonon. Thus, the β component may be composed of a couple of surface phonon modes. In fact, Chang *et al.* have found four surface phonon modes for GaAs(100)-(4×1)-Ga and $-(1\times6)$-As surfaces.[10] They determined the frequencies of the surface phonon modes by fitting globally the data taken under different azimuth angles and pump polarization conditions. Following their results, it is conceivable that a couple of surface phonon modes contribute to the TRSHG signals in this work on the GaAs(100)-$c(8\times2)$ surface. However, it is impossible to determine uniquely a set of frequencies of phonon modes by fitting the limited data available in this study. Therefore, we focus on the overall feature of the β component without further spectral decomposition.

Since there are no theoretical works available on the surface phonon modes at the GaAs(100)-$c(8\times2)$ surface, we are forced to speculate what kind of surface phonon modes are responsible for the β component. A recent LEED *I-V* analysis showed that the GaAs(100)-$c(8\times2)$ reconstructed surface consists of rows in the [0-11] direction in which three adjacent Ga dimers are separated by one missing dimer.[19] From the hyper-Raman selection rule, the allowed modes in the present detection configuration ($p_{\rm in}$-$p_{\rm out}$, incidence plane $\|$[0-11]) are those with A_1 or B_2 symmetry.[10] Among the six normal modes of the Ga dimer, there are three allowed modes which would contribute to the β component: an out-of-plane mode of two Ga atoms in phase (A_1), an in-plane mode of two Ga atoms in opposite directions along the dimer bond (A_1), and an in-plane mode of two Ga atoms in phase along the axis perpendicular to the dimer bond (B_2).

Chang *et al.*[10] found four surface phonon components at 8.15, 7.80, 7.46, and 6.46 THz for the GaAs(100)-(4×1)-*Ga* surface. Since the highest frequency is close to that of the β component found in the current study, their modes are likely very similar. In Ref. 10, the authors assigned the component at 8.15 THz to an out-of-plane counter-propagating mode of the Ga-As bond between a Ga dimer and As atoms in the second layer, whose frequency is higher than that of the intrinsic mode because of coupling with the electric field associated with the displacement. The similar surface phonon mode should be at the GaAs(100)-$c(8\times2)$ surface, and is supposed to be the origin of the main feature of the β component. The motions of the Ga dimers in the phonon modes are with A_1 or B_2 symmetry as discussed above. Both the GaAs(100)-$c(8\times2)$ and the GaAs(100)-(4×1)-Ga surfaces are dominated by the local (4×2) structure. The difference between the two structures is that the (4×2) cells are staggered regularly over a wide region in the former reconstruction, while this arrangement is disordered in the latter.[20] This difference in the structure would be the reason why the surface mode frequencies at these surfaces do not coincide exactly.

Among the three other modes identified at the GaAs(100)-(4×1)-Ga surface by Chang *et al.*, the components at 7.46 and 6.46 THz are assigned to the modes localized at the third and forth layers because the deduced decay times (around 1 ps) are relatively longer than those of other modes.[10] These modes should exist at the GaAs(100)-$c(8\times2)$ surface in the similar frequency range. Note that some components appear at 6.0–7.6 THz in Fig. 4(b), while their relative intensity diminishes in Fig. 4(d). One possible explanation for this can be as follows. Since the phonon modes at 6.0–7.6 THz are localized at the third and fourth layers, these modes may not be so sensitive to the annealing time.

On the other hand, the majority of the β component is contributed from the motion of the Ga dimer with respect to the second layer, which is expected to be very sensitive to the homogeneity in the topmost layer. As increasing the annealing time, the surface homogeneity is improved and thereby contributions of the β component dominate the signal.

Note that a broad component at around 10 THz in Fig. 5 grows as the pumping power increases. It is not likely due to phonon modes, since no surface phonons possess frequency higher than that of the bulk LO phonon at the Brillouin zone center. Thus, we attribute the broad component to the contributions from photocarriers. The bulk photocarriers in the near surface region are not responsible for this component, since the wavefunctions of bulk free carriers decay to zero toward surface. Therefore, this component might be due to plasmon oscillations originating in photocarriers trapped in the surface states of GaAs(100)-$c(8\times2)$ above the Fermi level.

Here we discuss the initial phases of the observed modes. We observed the surface phonon components exhibit different initial phases from that of the bulk LO-phonon component. The initial phase of a coherent phonon oscillation depends on its excitation mechanism.[4] Mechanisms for coherent optical phonon excitation are categorized as either a Raman or a non-Raman process. In the Raman process, the initial phase of coherent nuclear motion depends on the detuning of laser photon energy from the resonant energy for an electronic transition. It is claimed that the driving force is purely displacive for $|\omega_R-\omega_0|\ll\delta_R$, but impulsive for $|\omega_R-\omega_0|\gg\delta_R$, where ω_R is the resonance frequency of the electronic transition, ω_0 is the excitation laser frequency, and δ_R is the width of the resonance.[4] Thus, in the former case, coherent nuclear motion is described as $\cos(\omega t)$, while in the latter case, it is described as $\sin(\omega t)$.

On the other hand, some non-Raman processes have been proposed to explain coherent phonon excitation in opaque solids.[3,21] One of the most prominent models is denoted as displacive excitation of coherent phonons (DECP), which is based on interband excitation from bonding to antibonding states. Since the lattice equilibrium position changes abruptly by the excitation, the coherent amplitude is modulated as $\cos(\omega t)$.[3] As for the space charge layer in semiconductors, another non-Raman mechanism for coherent bulk LO-phonon generation is well accepted, which is based on the ultrafast screening of a depletion field by photocarriers.[22] The initial phase of the nuclear motion induced by this mechanism is similar to that of DECP.

Following the discussion given in Ref. 22, the ultrafast screening of the depletion field at the GaAs(100)-$c(8\times2)$ surface is expected to be a dominant mechanism for driving the coherent bulk LO phonon. On the other hand, the phase difference between the α and the β components clearly indicates that the excitation mechanism of the surface component is different from that of the bulk phonon. In fact, Chang *et al.* have claimed that the surface phonon components are generated via the Raman process, since the relative contributions of the surface phonon modes depend on the pump polarization and the crystal azimuth angle in the light incidence plane.[8–10]

If the purely nonresonant Raman process were responsible for the surface phonon excitation, all the modes should show the $\sin(\omega t)$ oscillatory component, and the initial phases of the surface phonons would be shifted from that of the bulk phonon by $\pi/2$. However, since occupied and unoccupied surface electronic states are located close to the band gap of the GaAs surface,[23] the transition between the two states would couple to the resonant Raman excitation of the surface phonons. Therefore, the initial phases of the surface modes vary as a function of detuning of the photon energy from that of the relevant resonance. This might be why the relative phase between the α (bulk) and the β (surface) component does not match to $\pi/2$ exactly.

B. Excitation power dependence

In the above discussion, the β component is ascribed to the surface phonons confined in a few atomic layers. Here, we focus on the frequency shift of the β component as a function of the pump power. There are two possible origins for the frequency shift: (1) the softening of the bonds at the surface owing to excitation of the surface states and (2) the anharmonicity of the bonds at the surface.

If electrons (holes) are generated in antibonding (bonding) surface states by photoexcitation, the surface phonon modes are softened. A similar redshift of coherent bulk phonon frequency of tellurium as a function of pumping power has been reported.[24] The excitation of about 2% of valence electrons of bulk Tellurium causes the weakening of the crystal lattice and results in the low-frequency shift from 3.6 to 3.0 THz. In the present case, although the bulk carrier density is too low to modify the bulk phonon frequency, the two-dimensional (2D) confined surface mode might be perturbed by the excess carrier density in the unoccupied surface states. Haight *et al.* have reported the electron dynamics in the surface states of GaAs(110) by time-resolved two photon photoemission spectroscopy.[25] The excited electrons in the surface states decay in a few picoseconds. Since the similar carrier dynamics in the surface states of GaAs(100)-$c(8\times2)$ can be expected, the photocarriers in the surface states survive sufficiently long to affect the surface phonon frequency.

Next we consider a possible role of the anharmonicity of surface bonds. As has been discussed earlier, the excitation mechanism of the coherent surface phonon on the GaAs surface is considered to be the impulsive Raman scattering.[8] In the classical damped oscillator picture, the amplitude of the induced oscillation would be proportional to the fluence of the excitation laser.[3] The coherent phonon amplitude becomes larger with increase of the excitation power, and finally the redshift of the phonon frequency is expected by the anharmonicity of the potential at the surface. Therefore, another possibility for the redshift is due to the anharmonicity of surface bonds.

Generally, the anharmonicity of surface phonon modes is considered to be greater than that of bulk phonon modes. Baddorf *et al.* have revealed that the anharmonicity for the motion normal to the surface on a Cu(110) surface, is 4–5 time greater than that in bulk copper.[26] However, little is

known about the anharmonic constants of the bonds at the GaAs surface. Verma *et al.* studied in detail the anharmonicity of the GaAs bulk LO phonon by temperature-dependent Raman scattering.[27] The LO-phonon line center frequency shifts from 297.5 cm^{-1} (8.92 THz) to 292 cm^{-1} (8.75 THz) as the temperature increases from 10 to 300 K. Following a formulation explored by Balkanski *et al.*, in which phonon coupling due to cubic and quartic anharmonic terms are taken into account,[28] they estimated the anharmonic constants from the temperature dependence of the peak frequency and the line width.

Chang *et al.* have suggested that the coherent phonon amplitudes observed at the surface and in the bulk are the same order of magnitudes on the GaAs.[10] Since the excitation conditions in this study are close to those in Ref. 10, the situation would be similar. Since the α component (bulk LO phonon) does not show significant power dependence of its frequency, the employed pump power is not so intense as to realize the anharmonic effect in the bulk. As in Fig. 5, the β component frequency shifts from 8.6 to 8.3 THz with the pump power changing from 70 to 210 mW. This shift is larger than that of the bulk mode observed between at 10 and 300 K, in which occupation at the phonon mode of 300 cm^{-1} increases from $\sim$0 to 0.3. It is intriguing that such a large shift is induced with the moderate pump power conditions. This could be a manifestation of larger anharmonicity at the surface than that in the bulk.

V. CONCLUSION

We performed TRSHG measurements on a GaAs(100)-$c(8\times2)$ surface, and identified the surface phonon mode in the time domain. The surface phonon signals show dramatic dependence on the surface annealing, which indicates that the observed mode is sensitive to the long-range regularity of the surface. Clear interference dips were observed in the power spectra, which are indicative of the initial phase difference between the bulk and the surface phonon modes. The surface phonon frequency showed a red-shift as the pump power increases. This might be ascribed to the change of the interatomic force constant by the photocarriers in the antibonding unoccupied surface state, or to the anharmonicity of the potential energy curve for the surface lattice motion.

ACKNOWLEDGMENTS

This work was supported in part by the Grants-in-aid for Scientific Research by Japan Society for the Promotion of Science (JSPS) (Grant Nos. 11304041, 12874086, and 13874068). K.W. is grateful for the financial support from The Kao Foundation For Arts And Sciences. D.T.D. is also grateful to JSPS for financial support.

*Corresponding author. E-mail address: matsumoto@soken.ac.jp

[1] J. C. Polanyi and A. H. Zwail, Acc. Chem. Res. **28**, 119 (1995).
[2] Y. Yan and K. A. Nelson, J. Chem. Phys. **87**, 6240 (1987); **87**, 6257 (1987).
[3] T. Dekorsy, G. C. Cho, and H. Kurz, in *Light Scattering in Solids VIII*, edited by M. Cardona and G. Güntherodt (Springer-Verlag, Berlin, 2000), pp. 169–209.
[4] R. Merlin, Solid State Commun. **102**, 207 (1997).
[5] A. M. Weiner, D. Leaird, and K. A. Nelson, J. Opt. Soc. Am. B **8**, 1264 (1991).
[6] M. Hase, K. Mizoguchi, H. Harima, S. Nakashima, M. Tani, K. Sakai, and M. Hangyo, Appl. Phys. Lett. **69**, 2474 (1996).
[7] M. Hase, T. Itano, K. Mizoguchi, and S. Nakashima, Jpn. J. Appl. Phys. **37**, L281 (1998).
[8] Y. M. Chang, L. Xu, and H. W. K. Tom, Phys. Rev. Lett. **78**, 4649 (1997).
[9] Y. M. Chang, L. Xu, and H. W. K. Tom, Phys. Rev. B **59**, 12 220 (1999).
[10] Y. M. Chang, L. Xu, and H. W. K. Tom, Chem. Phys. **251**, 283 (2000).
[11] T. A. Germer, K. W. Kolasiñski, J. C. Stephenson, and L. J. Richter, Phys. Rev. B **55**, 10 694 (1997).
[12] W. E. Bron, J. Kuhl, and B. K. Rhee, Phys. Rev. B **34**, 6961 (1986).
[13] G. C. Cho, W. Kütt, and H. Kurz, Phys. Rev. Lett. **65**, 764 (1990).
[14] G. C. Cho, T. Dekorsy, H. J. Bakker, R. Hövel, and H. Kurz, Phys. Rev. Lett. **77**, 4062 (1996).
[15] M. Hase, K. Mizogushi, H. Harima, F. Miyamaru, S. Nakashima, R. Furusawa, M. Tani, and K. Sakai, J. Lumin. **76–77**, 68 (1998).
[16] K. Wan and J. F. Young, Phys. Rev. B **41**, 10 772 (1990).
[17] F. Stietz, J. A. Schaefer, and A. Goldmann, Surf. Sci. **383**, 123 (1997).
[18] R. Fuchs and K. L. Kliewer, Phys. Rev. **140**, 2076 (1965).
[19] J. Cerdá, F. J. Palomares, and F. Soria, Phys. Rev. Lett. **75**, 665 (1995).
[20] P. Kraus, W. Nunes Rodrigues, and W. Mönch, Surf. Sci. **219**, 107 (1989).
[21] H. J. Zeiger, J. Vidal, T. K. Cheng, E. P. Ippen, G. Dresselhaus, and M. Dresselhaus, Phys. Rev. B **45**, 768 (1992).
[22] T. Pfeifer, T. Dekorsy, W. Kütt, and H. Kurz, Appl. Phys. A: Mater. Sci. Process. **55**, 482 (1992).
[23] Y.-C. Chang and D. E. Aspnes, Phys. Rev. B **41**, 12 002 (1990).
[24] S. Hunsche, K. Wienecke, T. Dekorsy, and H. Kurz, Phys. Rev. Lett. **75**, 1815 (1995).
[25] R. Haight and J. A. Silverman, Phys. Rev. Lett. **62**, 815 (1989).
[26] A. P. Baddorf and E. W. Plummer, Phys. Rev. Lett. **66**, 2770 (1991).
[27] P. Verma, S. C. Abbi, and K. P. Jain, Phys. Rev. B **51**, 16 660 (1995).
[28] M. Balkanski, R. F. Wallis, and E. Haro, Phys. Rev. B **28**, 1928 (1983).